Bone ingrowth of various porous titanium scaffolds produced by a moldless and space holder technique: an *in vivo* study in rabbits

2016 Biomed. Mater. 11 015012

(http://iopscience.iop.org/1748-605X/11/1/015012)

Biomedical Materials

PAPER

Bone ingrowth of various porous titanium scaffolds produced by a moldless and space holder technique: an *in vivo* study in rabbits

Widyasri Prananingrum[1], Yoshihito Naito[2], Silvia Galli[3], Jiyoung Bae[4], Kazumitsu Sekine[4], Kenichi Hamada[4], Yoritoki Tomotake[2], Ann Wennerberg[3], Ryo Jimbo[3] and Tetsuo Ichikawa[1]

[1] Department of Oral and Maxillofacial Prosthodontics and Oral Implantology, Institute of Biomedical Sciences, Tokushima University Graduate School, Tokushima, Japan
[2] Oral Implant Center, Tokushima University Hospital, 3-18-15 Kuramoto, Tokushima, 770-8504, Japan
[3] Department of Prosthodontics, Faculty of Odontology, Malmö University, Malmö, Sweden
[4] Department of Biomaterials and Bioengineering, Institute of Biomedical Sciences, Tokushima University Graduate School, Tokushima, Japan

E-mail: yoshi11@tokushima-u.ac.jp

RECEIVED
17 April 2015

REVISED
28 October 2015

ACCEPTED FOR PUBLICATION
2 November 2015

PUBLISHED
2 February 2016

Keywords: biomaterials, animal study, bone substitutes, histological analysis

Abstract

Porous titanium has long been desired as a bone substitute material because of its ability to reduce the stress shielding in supporting bone. In order to achieve the various pore structures, we have evolved a moldless process combined with a space holder technique to fabricate porous titanium. This study aims to evaluate which pore size is most suitable for bone regeneration using our process. The mixture comprising Ti powder, wax binder and PMMA spacer was prepared manually at 70 °C which depended on the mixing ratio of each group. Group 1 had an average pore size of 60 μm, group 2 had a maximum pore size of 100 μm, group 3 had a maximum pore size of 200 μm and group 4 had a maximum pore size of 600 μm. These specimens were implanted into rabbit calvaria for three and 20 weeks. Thereafter, histomorphometrical evaluation was performed. In the histomorphometrical evaluation after three weeks, the group with a 600 μm pore size showed a tendency to greater bone ingrowth. However, after 20 weeks the group with a pore size of 100 μm showed significantly greater bone ingrowth than the other groups. This study suggested that bone regeneration into porous titanium scaffolds is pore size-dependent, while bone ingrowth was most prominent for the group with 100 μm-sized pores after 20 weeks *in vivo*.

1. Introduction

Oral implant treatment has become an established alternative in dentistry, and the treatment success over 5 years or more may be higher than 95% [1]. Today, the clinical challenge is to increase the success of implant treatment in compromised situations, such as atrophied bone, radiated bone or reconstructed bone after tumorectomy [2, 3]. In these cases, patients often lack sufficient bone support to maintain the stability of the implant and thus massive bone augmentation therapy is often conducted. Bone substitutes such as calcium phosphate materials are utilized in relatively small defects, however, in the case of larger defects, such as a resected jawbone, metallic materials such as titanium plates may be preferable because of their mechanically superior characteristics. However, the superior mechanical properties of titanium-based materials can also be a problem under functional loading, since the mismatch of the mechanical properties between the implant and the bone can result in stress shielding in the supporting bone [4, 5]. One of the methods used to overcome this issue is the application of porosity to the titanium material. This modification has been reported to reduce the discrepancy between the mechanical properties of the bone and the material [6]. Moreover, the bone integrates into the pore structure of the titanium, which provides a high interlocking capacity between the bone and the titanium [7].

Several methodologies exist to produce porous titanium structures, such as hot isostatic pressing (HIP) [8], metal injection molding (MIM) [9], 3D printing and spark plasma sintering (SPS) [10]. Unfortunately, it must be noted that some of the methods are complicated, incapable of producing an arbitrarily shaped prosthesis or costly at present.

We previously introduced a moldless technique to produce a tailored porous titanium material [11].

A drawback with this technique was that it was difficult to control the pore size of the porous titanium. Since pore morphology (e.g. size and interconnectivity) is known to be an important factor for protein adsorption, cellular migration [12, 13] and osteoconduction [14, 15], the maintenance of an optimal pore size may be of great importance [16, 17]. It has been reported that bone ingrowth into porous structures is optimal when the pore size is around 50 μm [18], whereas higher amounts of mineralized bone are present within the porous structure when the pore size is larger than 100 μm [19].

One of the useful approaches to control pore size is the space holder method, a common industrial method that works by mixing spacer materials that disappear during a heating process such as debindering and sintering [20]. In this study, we evolved our moldless process and combined it with the space holder technique to produce a titanium scaffold that can control pore size. In order to evaluate which pore size is most suitable for bone regeneration, different pore sizes were produced and tested *in vivo* using a calvarial defect of the rabbit.

2. Materials and methods

2.1. Specimen preparation

Commercially pure Ti powder (diameter $<$150 μm; Osaka Titanium Technologies Co., Tokyo, Japan) was utilized for the control group and smaller Ti powder ($<$325 mesh; Nilaco Co., Tokyo, Japan) was utilized for the test groups. The size of the $<$325 mesh is equivalent to $<$45 μm. Porous titanium discs were prepared for the study in the following manner: for evaluation of the mechanical properties, diameter 6 mm and height 10 mm; and for the *in vivo* study, diameter 5 mm and height 2 mm.

The control specimen was fabricated using a moldless process without a space holder, in line with our previous study. An inlay casting wax (custom ordered colorless type I; GC Corporation, Tokyo, Japan) was used as a binder to maintain the form until initial sintering. Thereafter, 90 wt% titanium powder and 10 wt% wax were mixed and shaped manually at 70 °C on a hot plate to obtain a green compact [11].

For the test groups, the moldless/space holder combined technique was utilized. PMMA powder (GC Corporation, Tokyo, Japan) was used as the space holder. Ti powder, PMMA powder and inlay casting wax were mixed and shaped as the control group, following the ratio presented in table 1. After preparing the green compacts, the specimens were heated in air at a rate of 20 °C min^{-1} up to 380 °C for 2 h to remove the binder without a mold. Thereafter, sintering was conducted in an argon atmosphere at a heating rate of 10 °C min^{-1} to 1100 °C for 1 h. The sintered specimens were ultrasonically cleaned with acetone, ethanol and distilled water for 10 min progressively. Finally, the specimens were dried in a desiccator overnight.

2.2. Characterization of the produced sintered specimens

Sintering progress and pore morphology were confirmed by scanning electron microscopy (SEM; JCM-5700, JEOL, Tokyo, Japan). The total porosity of the specimens was evaluated on the basis of the apparent volume calculated from the specimen dimensions and the actual volume was evaluated via helium pycnometry (Accupyc II 1340, Micromeritics Instrument Corp., Norcross, USA) using the method presented by Semel and Lados [21]. Pore size distribution was measured using an automated mercury porosimeter (Autopore 9400, Micromeritics Instrument Corp., Norcross, USA). In order to measure the pore size shrinkage, the 3D pore size was examined using a micro-CT scanner (SkyScan1176, Bruker MicroCT, Belgium). All scans were obtained at 90 kV and 270 μA, using an aluminum–copper filter to optimize the contrast, and had a pixel size of 17.59 μm. All data were exported in an image file format and were imported into analysis software (CTAn v 1.14.4.1, Bruker MicroCT, Belgium) for the measurement of pore size before and after sintering. The pore size shrinkage was calculated from measured values (figure 5). The elastic modulus was evaluated using a universal testing machine (AG-X series, Shimadzu, Kyoto, Japan) in compression tests. The crosshead speed was 0.5 mm min^{-1}. Electrical resistance gauges (base width: 2 mm; base length: 3 mm) were mounted on four lateral side surfaces to measure the longitudinal elastic strain under compression.

2.3. Surgical procedure

12 mature New Zealand White rabbits (weight: 3.3–4.2 kg) were used for the study, following the Ethics Committee for Animal Research at the École Nationale Vétérinaire d'Alfort (Maisons-Alfort, Val-de-Marne, France). All surgical procedures were performed under general anesthetic using ketamine chlorate and the vital signs were monitored throughout the surgery.

After shaving and aseptic treatment of the surgical sites with iodine solution, a linear 5 cm incision was made on the calvarium and full-thickness flaps were raised. Four bone defects of 5 mm in diameter were created using a trephine bur with sterile saline irrigation. In these created defects, titanium porous disks of different pore sizes (as mentioned previously) were placed randomly. Thereafter, the muscle layers and skin were sutured with a resorbable suture (Vicryl, Ethicon, Auneau, France). The animal pain and discomfort were minimized via analgesic therapy; a patch of Fentanyl 4 μg kg^{-1} h^{-1} was applied to the animal skin for three days after the operation and meloxicam 0.2 mg kg^{-1} was administered intramuscularly before anesthesia and then every day for five days post-operation. Antibiotic therapy was carried out, with enrofloxacine dispersed in the drinking water of the animal (a dose of 200 mg^{-1} l^{-1} of water) for five days.

2.4. Histological preparation

After three and 20 weeks of healing, the animals were euthanized via an anesthesia overdose and the

Table 1. Mixing ratio of Ti powder, wax binder and PMMA spacer.

	PMMA powder size (μm)	Ti powder (mass %)	Wax binder (mass%)	PMMA spacer (mass %)
Group 1 (control)	—	90	10	—
Group 2	100	75	12	13
Group 3	200	75	12	13
Group 4	600	78	12	10

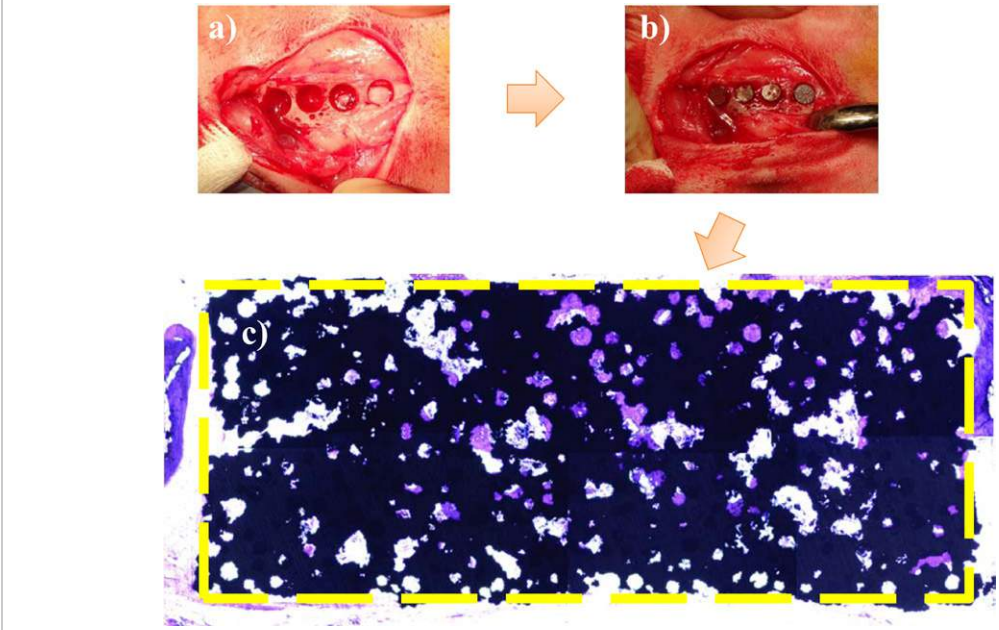

Figure 1. Surgical procedures. Four bone defects were created (a). The defects were filled with bone cement according to group (b). Histological analysis was perfomed (c).

specimens were removed *en bloc* and subsequently perfused in 4% formaldehyde for 24 h. After fixation, the samples were dehydrated in a series of ethanol (70%–100%) and infiltrated into light curable resin (30%–100%; Technovit 7200 VLC, Heraeus Kulzer Wehrheim, Germany) under vacuum conditions. After complete infiltration, the samples were embedded in a new 100% resin. The embedded resin blocks were subjected to non-decalcified cut and grind sectioning to a final thickness of 30 μm and were then stained with toluidine blue and pyronin G.

The histological analyses were performed using a light microscope (Eclipse ME600, Nikon, Japan) and the histomorphological data were analyzed using Image J (National Institutes of Health, USA). The total amount of newly generated bone within the defect was calculated as a percentage using a $\times 10$ magnification objective (figure 1).

2.5. Statistical analysis

The statistical analysis was performed using a non-parametric Kruskal–Wallis test followed by a Bonferroni *post hoc* test for multiple comparisons using the computer software SPSS (SPSS Inc., Chicago, IL, USA). Statistical significance was set at 95%.

3. Results

3.1. Mechanical property

The SEM image of the tested specimen is presented in figure 2. The majority of the pore sizes were comparable to that of the PMMA particle used for spacers.

As shown in figure 3, porosities in the range 38.48–43.07% were successfully obtained. The total porosity of the porous titanium cylinder after sintering was based on the apparent volume calculated from the specimen dimensions and the actual volume evaluated using helium pycnometry. There was no significant difference in porosity between the groups ($p < 0.05$). The porosity of the control group was 38.48% and for the test groups it was in the range 40.52–43.07%.

Figure 4 shows the pore size distributions for each specimen. It could be suggested that the small pore diameters had a similar distribution in all the groups. From the pore size shrinkage test (figure 5), the shrinkage of group 4 was significantly lower than that of groups 2 and 3 ($p < 0.05$). The pore sizes that we created intentionally using the mixing PMMA spacer were 103.1, 202.5 and 610.8 μm in groups 2, 3 and 4, respectively. In addition, the elastic modulus produced by our method is shown in figure 6. The Young's modulus of the control group was 17.77 GPa and for the test groups

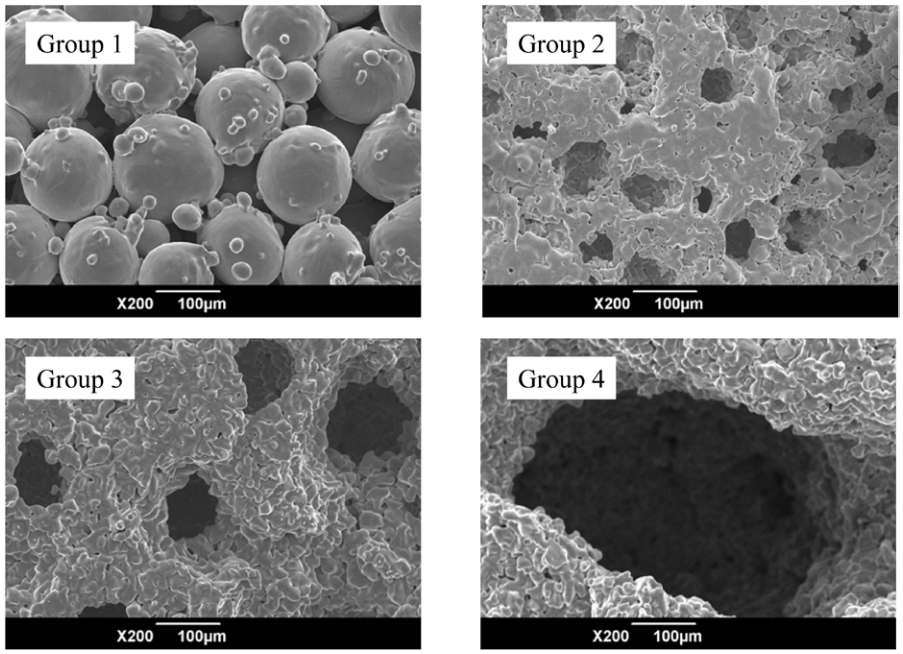

Figure 2. SEM images of the different pore sizes of the porous titanium after sintering.

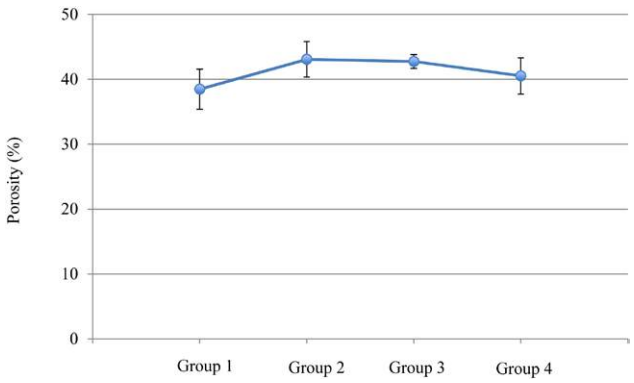

Figure 3. Porosity of the various porous titanium scaffolds.

it was in the range 28.05–35.61 GPa. Although no differences between the test groups were detected ($p < 0.05$), there were significant differences between the control group and the test groups.

3.2. Histological analysis

After three and 20 weeks *in vivo*, new bone formation was observed in all of the groups. The newly formed bone grew into the pores and at the implant–bone interface (figures 7 and 8). There were no significant differences between the groups after three weeks of healing. At 20 weeks, group 2 (10.27 ± 3.00%) presented a significantly higher bone area than groups 1 (5.43 ± 2.22%) and 4 (6.21 ± 2.04%), but groups 2 and 3 (7.56 ± 1.51%) showed no statistical differences (figure 9).

4. Discussion

In this study, we have evaluated the bone ingrowth capabilities of porous titanium scaffolds with various pore sizes prepared using a moldless process combined with a space holder method. Titanium has a long history of use with regards to biomaterials and its combination of excellent biomechanical and biocompatible properties has enabled applications in numerous areas of the human body, in particular for the replacement of hard tissues. The use of calcium phosphate-based scaffolds has traditionally been preferred [22], but the mechanical stability of the scaffolds has been raised as a potential drawback [23]. External pressure from soft tissue has been one of the causes of bone graft resorption, especially in external bone grafting situations such as veneer grafting. Thus, titanium-based non-resorbable scaffolds, where the influence of external tension can be minimized, have been of some interest [7, 24, 25].

The material characterization suggested that the methodology applied in this study could consistently produce the intended porous titanium devices with good formability. The porous titanium contains two types of pores: small pores, formed by the particle of titanium

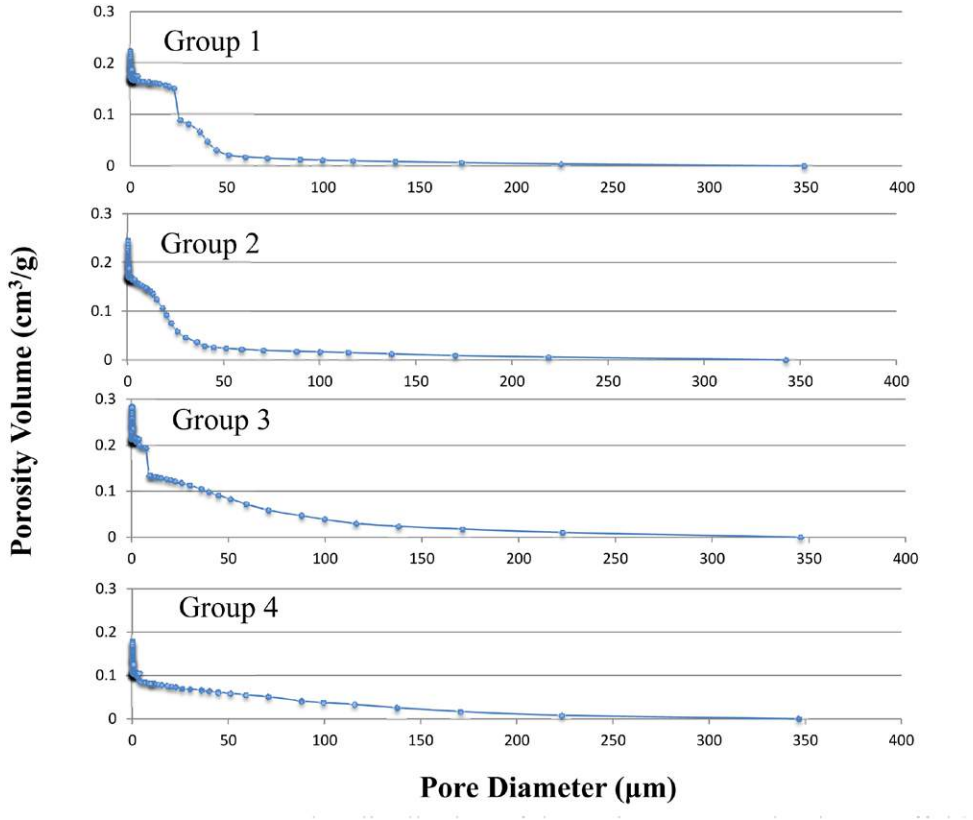

Figure 4. Pore size distribution of the various porous titanium scaffolds.

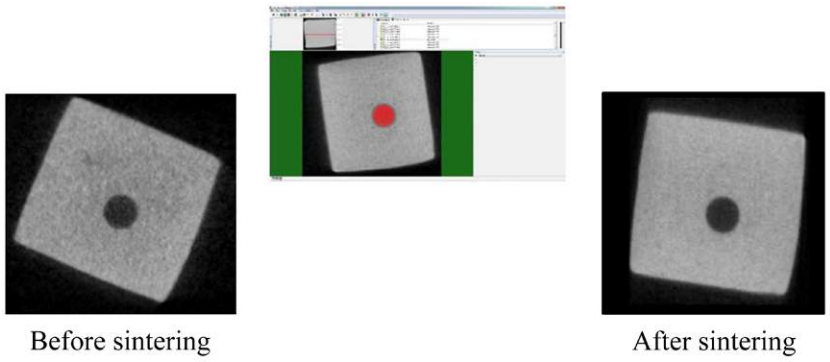

	Pore size before sintering (µm)	Pore size after sitering (µm)	Shrinkage of pore size (%)
Group2	130.6±9.4	103.1±6.6	20.9
Group3	251.3±34.7	202.5±16.6	18.8
Group4	708.6±31.6	610.8±28.5	13.8

Figure 5. Sintering effect for pore size and shrinkage.

powder, and large pores, determined by the size of the PMMA spacer. In this study, the distribution of the small pore sizes was similar in all the groups (figure 4). On the other hand, the large pore sizes, which were made using the PMMA spacer, were controlled so that there were significant differences in pore size between the different groups (figure 5). These results indicated that the small pore sizes and surface roughness are not associated with bone ingrowth, but the large pore sizes may have contributed to it. Moreover, the elastic modulus produced by the method utilized in this study presented values similar to that of the human cortical bone, ranging between 17.77–35.61 GPa. However, the different groups introduced in this study presented different mechanical values, which may have

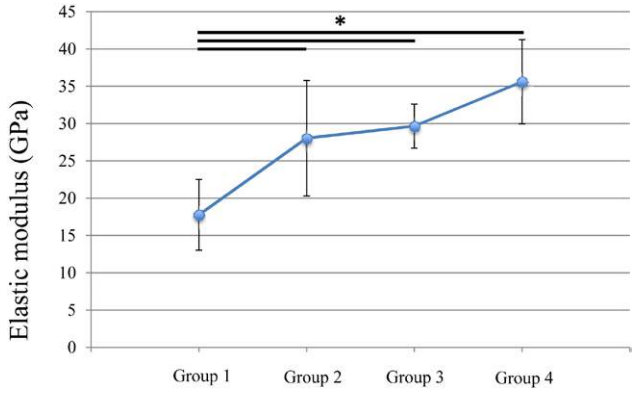

Figure 6. Elastic modulus of the porous titanium scaffolds according to group. *$p < 0.05$.

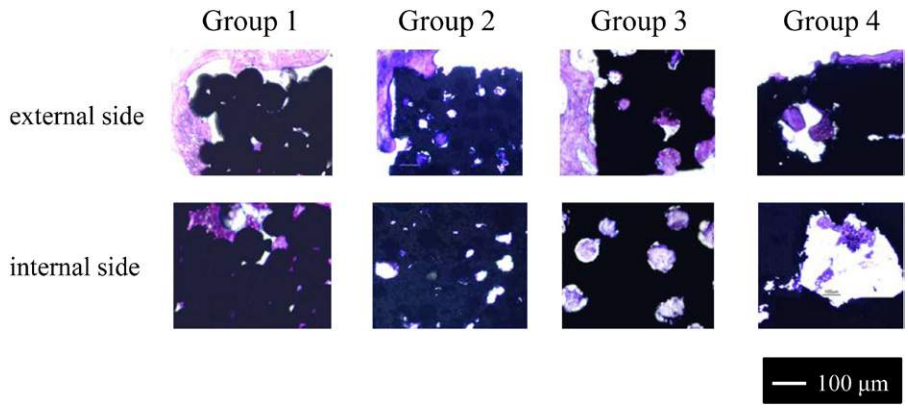

Figure 7. Histological images at three weeks.

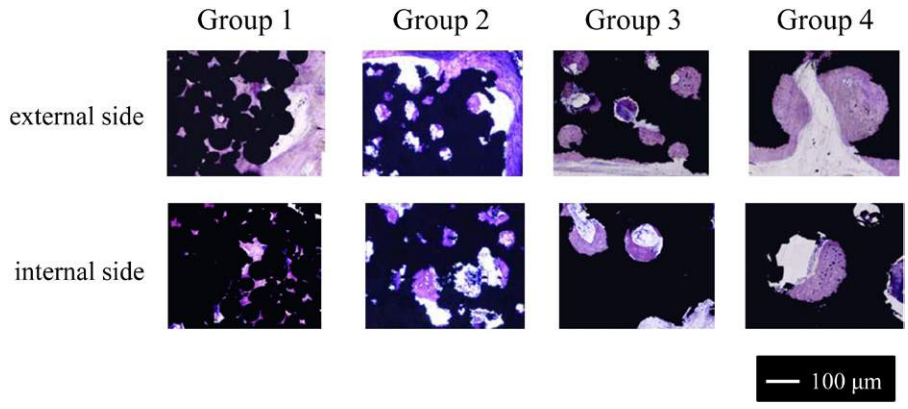

Figure 8. Histological images at 20 weeks.

been caused by the structural differences, as seen in the SEM images. These differences may be another reason for the different biologic outcomes, since the stiffness of the scaffolding material is an essential factor for bone regeneration [26].

The histologic analysis showed that regardless of the size of the pores, bone ingrowth occurred. However, the degree of bone infiltration into the porous blocks was dependent on the porosity and pore size, as a porosity of 47.63% with a pore size of 100 μm presented the highest porosity by a significant margin and showed significantly more bone ingrowth than the other groups. This can be explained by the fact that osteoblasts respond differently according to the porosity and pore size. It was reported by Ono *et al* that a beta tri-calcium phosphate porous block with a porosity of about 46% presented excellent bone ingrowth [15]. It was also suggested in the same study (and in other studies) that a firm scaffold which functions as a space maintainer is as important [24, 25].

In this study, bone ingrowth was observed after three and 20 weeks, providing insights into the duration of the bone regeneration process. With regard to the influence of pore size, it has been indicated that small pores favor hypoxic conditions and induced osteochondral forma-

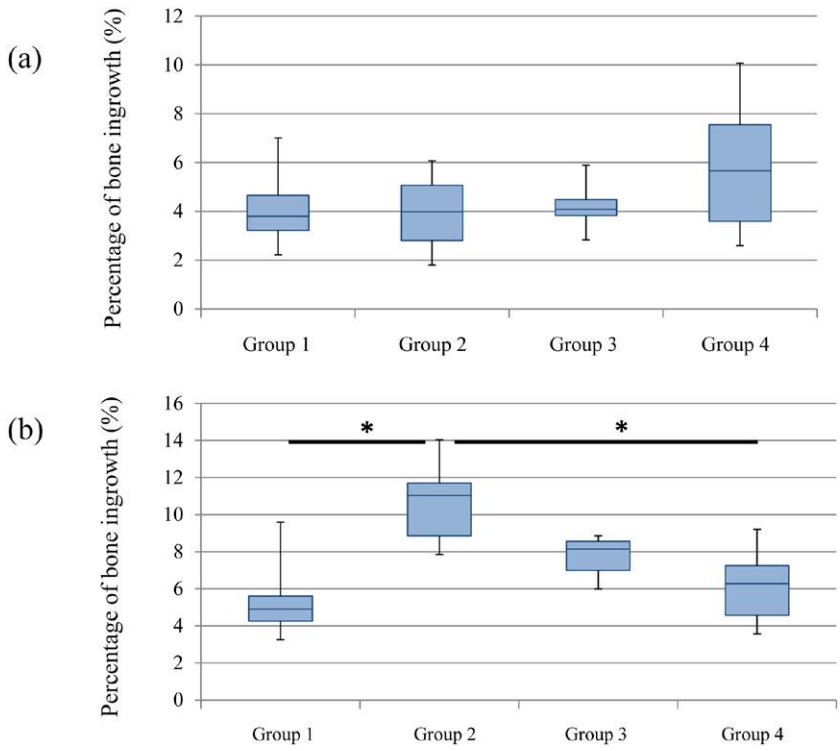

Figure 9. (a) Percentage of bone ingrowth after three weeks. (b) Percentage of bone ingrowth after 20 weeks. *$p < 0.05$. Values are shown as the mean.

Table 2. Surface roughness of specimens before and after sintering.

	Sa (μm) ± SD		Sds (1 μm^{-2}) ± SD		Sdr (%) ± SD	
Sample	Before	After	Before	After	Before	After
Group 1 (control)	5.484 ± 0.625	6.256 ± 1.636	0.0732 ± 0.0043	0.0429 ± 0.0055	3546.91 ± 1483.36	2709.39 ± 787.29
Group 2	3.410 ± 0.534	3.160 ± 0.653	0.0620 ± 0.0031	0.0379 ± 0.0077	677.45 ± 176.64	437.62 ± 134.75
Group 3	2.491 ± 0.092	2.789 ± 0.694	0.0584 ± 0.0032	0.0485 ± 0.0123	355.20 ± 53.95	612.57 ± 443.59
Group 4	2.525 ± 0.106	3.096 ± 0.714	0.0533 ± 0.0011	0.0513 ± 0.0068	232.77 ± 81.69	609.42 ± 292.15

tion before osteogenesis, while larger pores permit direct osteogenesis with a rich vascularized structure in the pores [27]. This is in accordance with the results of the current study after three weeks *in vivo*. The group with a 600 μm pore size showed a tendency to greater bone ingrowth compared with the other groups at the early phase of the bone regeneration process.

The histomorphometrical results after 20 weeks, corresponding to the remodeling phase, presented a completely different trend. The pore size of 100 μm showed the greatest amount of bone ingrowth, and the rate of bone ingrowth significantly decreased as the pore size grew. It can be assumed that a larger pore size does not offer major advantages at the mature phase of bone regeneration. This finding is in agreement with that of Gotz *et al*, where the level of osseointegration for the implants with larger pores was lower than that of the implants with smaller pores [28].

It can be suggested from the results of this study that there seems to be a pore size-dependent bone healing kinetics. Within the limitations of this study, it was shown that a pore size of 100 μm offers the strongest bone responses after a period of 20 weeks *in vivo*. An optimal balance between the porosity and mechanical properties of the scaffold material may be an essential factor for stable bone regeneration.

5. Conclusion

The results of this study suggest that bone regeneration into the porous titanium scaffolds was pore size-dependent and that bone ingrowth was most prominent for the group with 100 μm-sized pores after 20 weeks *in vivo*. This study also provides some insight into how to achieve stable bone regeneration, with large pores possibly having a beneficial effect in the early stages due to vascular invasion and the facilitation of osteogenesis, but further studies are needed to determine the optimal pore size or shape for bone ingrowth.

Acknowledgments

The research leading to these results has received funding from KAKENHI Grant Number 26893179.

We would also like to acknowledge Dr Y Jinno for his technical assistance during the histological preparation.

Author contributions

Widyasri Prananingrum: concept/design, material characterization and analysis

Yoshihito Naito: study design, animal operation, histological preparation and analysis

Silvia Galli: animal operation, histological preparation and analysis

Jiyoung Bae, Kazumitsu Sekine and Kenichi Hamada: material design, preparation and mechanical property evaluation

Yoritoki Tomotake: data analysis and material concept

Ann Wennerberg: study design and data analysis

Ryo Jimbo: study design, animal operation and data analysis

Tetsuo Ichikawa: concept/ design and data analysis

References

[1] Jimbo R and Albrektsson T 2015 Long-term clinical success of minimally and moderately rough oral implants: a review of 71 studies with five years or more of follow-up *Implant Dent.* **24** 62–9

[2] Buddula A, Assad D A, Salinas T J, Garces Y I, Volz J E and Weaver A L 2011 Survival of turned and roughened dental implants in irradiated head and neck cancer patients: a retrospective analysis *J. Prosthet. Dent.* **106** 290–6

[3] Donos N and Calciolari E 2014 Dental implants in patients affected by systemic diseases *Br. Dent. J.* **217** 425–30

[4] Johansson P, Jimbo R, Kjellin P, Currie F, Chrcanovic B R and Wennerberg A 2014 Biomechanical evaluation and surface characterization of a nano-modified surface on PEEK implants: a study in the rabbit tibia *Int. J. Nanomed.* **9** 3903–11

[5] Lewallen E A, Riester S M, Bonin C A, Kremers H M, Dudakovic A, Kakar S, Cohen R C, Westendorf J J, Lewallen D G and van Wijnen A J 2015 Biological strategies for improved osseointegration and osteoinduction of porous metal orthopedic implants *Tissue Eng.* B **21** 218–30

[6] Barbas A, Bonnet A S, Lipinski P, Pesci R and Dubois G 2012 Development and mechanical characterization of porous titanium bone substitutes *J. Mech. Behav. Biomed. Mater.* **9** 34–44

[7] Vandeweghe S, Leconte C, Ono D, Coelho P G and Jimbo R 2013 Comparison of histological and three-dimensional characteristics of porous titanium granules and deproteinized bovine particulate grafts used for sinus floor augmentation in humans: a pilot study *Implant Dent.* **22** 339–43

[8] Bocanegra-Bernal M H 2004 Review hot isostatic pressing (HIP) technology and its applications to metals and ceramics *J. Mater. Sci.* **39** 6399–420

[9] Melli V, Juszczyk M, Sandrini E, Bolelli G, Bonferroni B, Lusvarghi L, Cigada A, Manfredini T and Nardo L D 2015 Tribological and mechanical performance evaluation of metal prosthesis components manufactured via metal injection molding *J. Mater. Sci. Mater. Med.* **26** 5332

[10] Sakamoto Y, Asaoka K, Kon M, Matsubara T and Yoshida K 2006 Chemical surface modification of high-strength porous Ti compacts by spark plasma sintering *Biomed. Mater. Eng.* **16** 83–91

[11] Naito Y, Bae J, Tomotake Y, Hamada K, Asaoka K and Ichikawa T 2013 Formability and mechanical properties of porous titanium produced by a moldless process *J. Biomed. Mater. Res.* B **101** 1090–4

[12] Murphy C M, Haugh M G and O'Brien F J 2010 The effect of mean pore size on cell attachment, proliferation and migration in collagen–glycosaminoglycan scaffolds for bone tissue engineering *J. Biomater.* **31** 461–6

[13] Miranda S C, Silva G A, Mendes R M, Abreu F A, Caliari M V, Alves J B and Goes A M 2012 Mesenchymal stem cells associated with porous chitosan–gelatin scaffold: a potential strategy for alveolar bone regeneration *J. Biomed. Mater. Res.* A **100** 2775–86

[14] Park J W, Kim E S, Jang J H, Suh J Y, Park K B and Hanawa T 2010 Healing of rabbit calvarial bone defects using biphasic calcium phosphate ceramics made of submicron-sized grains with a hierarchical pore structure *Clin. Oral Implants Res.* **21** 268–76

[15] Ono D, Jimbo R, Kawachi G, Ioku K, Ikeda T and Sawase T 2011 Lateral bone augmentation with newly developed tricalcium phosphate block: an experimental study in the rabbit mandible *Clin. Oral Implants Res.* **22** 1366–71

[16] Li J P, Habibovic P, van den Doel M, Wilson C E, de Wijn J R, van Blitterswijk C A and de Groot K 2007 Bone ingrowth in porous titanium implants produced by 3D fiber deposition *Biomaterials* **28** 2810–20

[17] Karageorgiou V and Kaplan D 2005 Porosity of 3D biomaterial scaffolds and osteogenesis *Biomaterials* **26** 5474–91

[18] Geetha M, Singh A K, Asokamani R and Gogia A K 2009 Ti based biomaterials, the ultimate choice for orthopaedic implants—a review *Prog. Mater. Sci.* **54** 397–425

[19] Bobyn J D, Pilliar R M, Cameron H U and Weatherly G C 1980 The optimum pore size for the fixation of porous-surfaced metal implants by the ingrowth of bone *Clin. Orthop. Relat. Res.* **150** 263–70

[20] Arifvianto B and Zhou J 2014 Fabrication of metallic biomedical scaffolds with the space holder method: a review *Materials* **7** 3588–622

[21] Semel F J and Lados D A 2006 Porosity analysis of PM materials by helium pycnometry *Powder Metall. I* **49** 173–82

[22] Zhang J, Liu W, Schnitzler V, Tancret F and Bouler J M 2014 Calcium phosphate cements for bone substitution: chemistry, handling and mechanical properties *Acta Biomater.* **10** 1035–49

[23] Babis G C and Soucacos P N 2005 Bone scaffolds: the role of mechanical stability and instrumentation *Injury* **36** S38–44

[24] Anderud J, Abrahamsson P, Jimbo R, Isaksson S, Adolfsson E, Malmstrom J, Naito Y and Wennerberg A 2015 Guided bone augmentation using ceramic space-maintaining devices: the impact of chemistry *Clin. Cosmetic Invest. Dent.* **7** 45–53

[25] Anderud J, Jimbo R, Abrahamsson P, Isaksson S G, Adolfsson E, Malmstrom J, Kozai Y, Hallmer F and Wennerberg A 2014 Guided bone augmentation using a ceramic space-maintaining device *Oral Surg. Oral Med. Oral Pathol. Oral Radiol.* **118** 532–8

[26] Lin C Y, Kikuchi N and Hollister S J 2004 A novel method for biomaterial scaffold internal architecture design to match bone elastic properties with desired porosity *J. Biomech.* **37** 623–36

[27] Chen Y J, Feng B, Zhu Y P, Weng J, Wang J X and Lu X 2009 Fabrication of porous titanium implants with biomechanical compatibility *Mater. Lett.* **63** 2659–61

[28] Götz H E, Müller M, Emmel A, Holzwarth U, Erben R G and Stangl R 2004 Effect of surface finish on the osseointegration of laser-treated titanium alloy implants *J. Biomater.* **25** 4057–64